

INVESTIGATION ON CENTRALITY MEASURES AND OPINION DYNAMICS IN TWO-LAYER NETWORKS WITH REPLICA NODES

A PREPRINT

 **Chi Zhao**

Saint Petersburg State University,
7/9 Universitetskaya nab.,
Saint Petersburg, 199034, Russia
st081292@student.spbu.ru

 **Elena Parilina**

Saint Petersburg State University,
7/9 Universitetskaya nab.,
Saint Petersburg, 199034, Russia
School of Mathematics and Statistics,
Qingdao University,
Qingdao, 266071, PR China
e.parilina@spbu.ru

June 28, 2024

ABSTRACT

We examine two-layer networks and centrality measures defined on them. We propose two fast and accurate algorithms to approximate the game-theoretic centrality measures and examine connection between centrality measures and characteristics of opinion dynamic processes on such networks. As an example, we consider a Zachary's karate club social network and extend it by adding the second (internal) layer of communication. Internal layer represents the idea that individuals can share their real opinions with their close friends. The structures of the external and internal layers may be different. As characteristics of opinion dynamic processes we mean consensus time and winning rate of a particular opinion. We find significantly strong positive correlation between internal graph density and consensus time, and significantly strong negative correlation between centrality of authoritative nodes and consensus time.

Keywords Opinion dynamics · Centrality measure · General concealed voter model · Zachary's karate club

1 Introduction

There are macroscopic and microscopic opinion dynamics models. Macroscopic models including Ising model [1], Sznajd model [2], voter model [3], concealed voter model (CVM) [4, 5], and macroscopic version of general concealed voter model (GCVM) [6] examine social networks using statistical-physical and probability-theoretical methods to analyze distribution of opinions.

Within GCVM [6], it is supposed that the individuals communicate in two layers (internal and external) and can interact in internal or private layer. The latter assumption is different from CVM, where individuals do not express their true opinions in internal layer.

Examples of microscopic models of opinion dynamics are DeGroot model [7], Friedkin-Johnsen (F-J) model [8], and bounded confidence models [9, 10]. In the F-J model, actors can also factor their initial prejudices into every iteration of opinion [11]. The models of opinion dynamics based on DeGroot and F-J models, and Markov chains with possibility to control agents' opinions are proposed in [12, 13, 14, 15]. The levels of influence and opinion dynamics with the presence of agents with different levels of influence is examined in [16, 17].

A bounded confidence model (BCM) is a model, in which agents ignore opinions that are very far from their own opinions [18, 19]. The BCM includes two essential models: the Deffuant-Weisbuch model (D-W) proposed in paper [10], and the Hegselman-Krause (H-K) model introduced in the work [9]. In the D-W model, two individuals are randomly chosen, and they determine whether to interact according to the bounded confidence [20].

The micro version of GCVN is introduced in [21], and the difference between macro and micro versions is that in the micro version we do not need to adjust the simulation program according to different network structures. As long as network structure is given, the program automatically produces simulations. Therefore, we can use this program to simulate real networks. But for the macro version, we should adjust the corresponding state transition formulae for different network structures.

Since network structure in GCVN is two-layer, it is interesting to examine how not only this structure in general, but also network characteristics, e.g. different centrality measures [22], affect opinion dynamics and resulting opinion in consensus if it is reached. We consider two key performance indicators of opinion dynamics, namely, winning rate and consensus time.

Social power (influence centrality) is a concept that ranking the importance of nodes in a network. Centrality measures are used to identify the most powerful nodes in a network. Understand the powerful nodes is very important for opinion dynamics, which can help us to know which nodes play a crucial position for spreading the opinion. The most common centrality measures are betweenness centrality [23], closeness centrality [24, 25, 26] and degree centrality [27]. There are also some centrality measures based on random walk, such as random walk occupation centrality [28] which is the frequency of a node in the network being accessed during a random walk; random walk betweenness centrality [29] – the proportion of the path through a node to all paths during a random walk, random walk betweenness centrality does not depend on the shortest path, therefore it is more general than betweenness centrality; Random walk closeness centrality – a variant of closeness centrality [28], the computation of random walk closeness centrality is based on the mean first-passage time (MFPT). The analytical expressions of random walk based centrality measures can be found in [28]. Game-theoretic network centrality is a flexible and sophisticated approach to identify the most powerful nodes in a network, the root is from cooperative game theory, MK Tarkowski provide a good review for game-theoretic network centrality in [30]. The Shapley value [31] and the Myerson value [32] are both concepts from cooperative theory which is used to fairly distribute the total payoff among players based on their marginal contribution. In the paper [33], the authors introduce how to use Shapley value to determine the top-k nodes in the social network. Mazalov et al. proposed a game-theoretic centrality measure for weighted graph based on Myerson value in [34]. In [35], Mazalov and Khitraya propose a modified Myerson value for unweighted undirected graphs. This characteristic function of this modification considers not only for simple paths but also includes cycles. The next work of [35] is [36], where the authors introduce the concept of integral centrality for unweighted directed graph and provide a rigorous mathematical proof that this centrality measure satisfies the Boldi-Vigna axioms [37].

In this paper, firstly we extended our previous work in [38] by adding more centrality measures and examining the connection between centrality measures and opinion dynamics, and secondly we proposed two fast and accurate algorithms to approximate the game-theoretic centrality measures and examined them in randomly generated network and Zachary’s karate club network. The primary conclusion drawn from this research indicates that there is a significantly strong positive correlation between internal graph density and consensus time, and significantly strong negative correlation between centrality of authoritative nodes and consensus time. Our proposed algorithms effectively approximate the Shapley and Myerson values in randomly generated networks with high accuracy. Additionally our algorithms successfully determine the top-2 influential nodes in Zachary’s karate club network.

The rest of this paper is organized as follows. Section 2 introduces multi-layer network with replica nodes. Network properties are discussed in Section 3. Section 4 presents simulation experiments and results. We briefly conclude and discuss our future work in Section 5.

2 Multi-layer network with replica nodes

2.1 Multi-layer network

A multilayer network is a network formed by several networks that evolve and interact with each other. [39]

2.2 Replica nodes

In a multilayer network with replica nodes there is a one-to-one mapping of the nodes in different layers and corresponding nodes are called replica nodes. Since there is a one-to-one mapping between the nodes in different layers, every layer is formed by the same number of nodes. [39]

2.3 Two-layer network with replica nodes

We use the following notations to define a two-layer (external and internal) network with replica nodes:

1. N : number of nodes in each layer;
2. $a_i = (a_i^E, a_i^I)$: one-to-one mapping of node i in the external and internal layer, where a_i^E (a_i^I) is a representation of node i in the external (internal) layer;
3. $G_E(\mathcal{V}_E, \mathcal{E}_E)$: predefined external network, where $\mathcal{V}_E = \{a_i^E\}$ and \mathcal{E}_E represent a set of individuals and set of edges in the external layer;
4. $G_I(\mathcal{V}_I, \mathcal{E}_I)$: predefined internal network, where $\mathcal{V}_I = \{a_i^I\}$ and \mathcal{E}_I represent a set of individuals and set of edges in the internal layer;
5. $\mathcal{E}_C = \{(a_i^E, a_i^I) | i = 1, \dots, N\}$: edges between replica nodes.

A two-layer network with N individuals/agents can be defined as¹:

$$G(\mathcal{V}, \mathcal{E}), \quad (1)$$

where $\mathcal{V} = \mathcal{V}_E \cup \mathcal{V}_I$, $|\mathcal{V}_E| = |\mathcal{V}_I| = N$, and $\mathcal{E} = \mathcal{E}_E \cup \mathcal{E}_I \cup \mathcal{E}_C$.

2.4 Two-layer network simplification

$G(\mathcal{V}, \mathcal{E})$ is composed of $G_E(\mathcal{V}_E, \mathcal{E}_E)$ and $G_I(\mathcal{V}_I, \mathcal{E}_I)$ connected by \mathcal{E}_C . Two-layer Networks can also be represented by an adjacency matrix. The adjacency matrix of a two-layer network is a block matrix, where the diagonal blocks are the adjacency matrices of the external and internal layers, and the off-diagonal blocks are the adjacency matrices of the connections between the external and internal layers.

The adjacency matrix of $G(\mathcal{V}, \mathcal{E})$ is shown in Equation 2.

$$A = \begin{bmatrix} A_{EE} & A_{EI} \\ A_{IE} & A_{II} \end{bmatrix} \quad (2)$$

Where, A_{EE} is the adjacency matrix of the external layer, A_{EI} is the adjacency matrix of the connections between the external and internal layers, A_{IE} is the adjacency matrix of the connections between the internal and external layers, and A_{II} is the adjacency matrix of the internal layer. For the undirected graph, the adjacency matrix A is symmetric.

It's possible to redefine a two-layer network $G(\mathcal{V}, \mathcal{E})$ to a one layer network with weight. We can define a fusion rule as follows:

$$W' = \pi_{c_e} \cdot A_{EE} + \pi_{c_i} \cdot A_{II} + \pi_i \cdot \Lambda_E + \pi_e \cdot \Lambda_I \quad (3)$$

Where Λ_E and Λ_I are diagonal matrices, and the elements on the diagonal represent the degrees of each node. Furthermore, we have a new weight network $G'(\mathcal{V}', \mathcal{E}', W')$, where $\mathcal{V}' = \{1, 2, \dots, N\}$ is the set of nodes in the new network, \mathcal{E}' is the set of edges in the new network, and W' is the weight matrix of the new network.

Based on the new weight network $G'(\mathcal{V}', \mathcal{E}', W')$, we proposed two game-theoretic centrality measures, we will discuss in the Section 3.3.

2.5 Zachary's karate club network in two-layer setting

As an example of a social network, we consider Zachary's karate club network representing friendship relations among 34 members of a karate club at the US university in the 1970s [41]. The study became famous in data and network analytical literature since it highlighted a conflict between manager (Node 0) and director (Node 33), which eventually led to the split of the club into two groups. One-layer Zachary's karate club network is represented in Fig. 1.

Fig. 2 shows how one-layer Zachary's Karate Club network can be extended into two-layer network if we add an internal layer of communication between agents. As discussed above, in CVM the nodes in the internal layer are not connected, i.e. internal layer is represented by an empty graph (Fig. 2a), while in GCVM there may be nonempty network representing internal communication of agents. In Fig. 2b we represent a star internal structure. The colors in Fig 2 represent individuals' opinions. The color, blue or red, is randomly initialized according to the given parameters ($\rho = 0.75$ for BVM and $\rho_{r_e} = 0.75, \rho_{r_i} = 0.25, \rho_r = 0.2$ for CVM and GCVM²).

¹This definition and the corresponding opinion dynamic models was firstly introduced in [21] and further discussed in [40] and [38].

² ρ represent the ratio of red opinion in the BVM network, ρ_{r_e} , ρ_{r_i} and ρ_r stand for ratio of red opinion in external, internal and both layer network respectively.

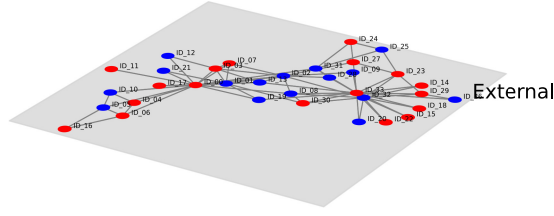
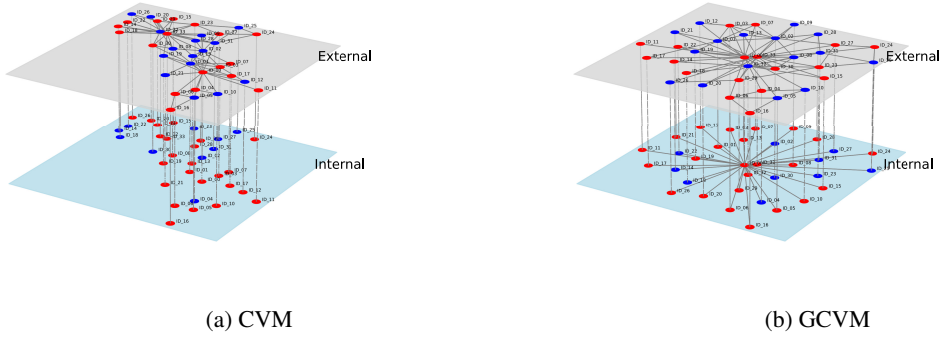


Figure 1: One-layer Zachary's karate club network



(a) CVM

(b) GCVM

Figure 2: Two-layer networks used in CVM and GCVM: (a) CVM: two-layer network with external Zachary's karate club and empty internal layer, (b) GCVM: two-layer network with external Zachary's karate club and star internal layer.

3 Centrality measures in one- and two-layer networks

In this section, we represent several centrality measures. Some of them are defined for one-layer networks and can be applied for two layers separately, some of them take into account the multi-layer structure of a network. We also introduce game-theoretical centrality measures and provide an algorithm to calculate their approximation when the network contains large number of nodes.

Definition 1 We define the pairwise average shortest path for an external layer d_E in two-layer network as follows:

$$d_E = \sum_{s,t \in \mathcal{V}_E} \frac{d_E(s,t)}{n_E(n_E - 1)}, \quad (4)$$

where $d_E(s,t)$ is a length of the shortest path between nodes s and t in external layer, \mathcal{V}_E is a set of nodes in external layer, $n = |\mathcal{V}_E|$ is a number of nodes in external layer. Similarly, we can define d_I as a pairwise average shortest path for an internal layer.

Definition 2 A graph density is a ratio of the number of edges $|\mathcal{E}|$ with respect to the maximal number of edges. Since internal layer is represented by an undirected graph, we define an internal graph density as in [42]:

$$D_I = \frac{2|\mathcal{E}_I|}{|\mathcal{V}_I|(|\mathcal{V}_I| - 1)}. \quad (5)$$

3.1 Classical Centrality measures

In this section we briefly introduce some (most well-known) centrality measures defined for one-layer networks.

3.1.1 Betweenness centrality

Betweenness centrality is a basic concept in a network analysis, which was suggested in [23]. Betweenness centrality of a node gives the number of geodesics between all nodes that contain this node. It reflects the level of node participation

in the dissemination of information between other nodes in a graph. It is calculated by the formula:

$$C_b(v) = \frac{1}{n_b} \sum_{s,t \in V} \frac{\sigma_{s,t}(v)}{\sigma_{s,t}}, \quad (6)$$

where $\sigma_{s,t}$ indicates the number of shortest paths between nodes s and t , and $\sigma_{s,t}(v)$ is the number of shortest paths between nodes s and t containing node v . Normalization coefficient is $n_b = (|V|-1)(|V|-2)$ for $v \notin \{s, t\}$, otherwise $n_b = |V|(|V|-1)$, where $|V|$ is the number of nodes in a one-layer network [22]. If $s = t$, $\sigma_{s,t} = 1$ and if $v \in \{s, t\}$, then $\sigma_{s,t}(v) = 0$.

3.1.2 Group betweenness centrality

Group betweenness centrality measure indicates a proportion of shortest paths connecting pairs of nongroup members that pass through the group [43], and it is defined by formula:

$$C_{gb}(X) = \frac{1}{n_{gb}} \sum_{s,t \in V \setminus X} \frac{\sigma_{s,t}(X)}{\sigma_{s,t}}, \quad (7)$$

where $\sigma_{s,t}(X)$ is the number of shortest paths between nodes s and t passing through some nodes in group X . Normalization coefficient is $n_{gb} = (|V| - |X|)(|V| - |X| - 1)$, where $|X|$ is the number of nodes in group X .

3.1.3 Closeness centrality

In a connected graph, closeness centrality of node u is the reciprocal of a sum of lengths of the shortest paths between u and all other nodes in the graph [24, 25, 26]. When calculating closeness centrality, its normalized form is usually referred to as the one representing the average length of the shortest path instead of their sum, and it is calculated like this:

$$C_c(u) = \frac{n_c}{\sum_{v \in V \setminus \{u\}} d(v, u)}, \quad (8)$$

where normalization coefficient is $n_c = |V| - 1$.

3.1.4 Group closeness centrality

Group closeness centrality is the reciprocal of the sum of the shortest distances from the group to all nodes outside the group [43, 44, 45]. It is defined by the formula:

$$C_{gc}(X) = \frac{n_{gc}}{\sum_{v \in V \setminus X} d(v, X)}, \quad (9)$$

where $d(v, X)$ is the shortest distance between group X and v . Normalization coefficient is $n_{gc} = |V - X|$.

3.1.5 Degree centrality

Degree centrality of node v [27] is defined as

$$C_d(v) = \frac{v_d}{n_d}, \quad (10)$$

where v_d is a degree of node v , and normalization coefficient is $n_d = |V| - 1$.

3.1.6 Group degree centrality

Group degree centrality is the number of nodes outside the group connected with the nodes from this group [43, 44]. Normalized group degree centrality for group X is given by the formula:

$$C_{gd}(X) = \frac{|\{v_i \in V \setminus X | v_i \text{ is connected to } v_j \in X\}|}{n_{gd}}, \quad (11)$$

where normalization coefficient is $n_{gd} = |V| - |X|$.

3.2 Random walk based centralities

The second group of centrality measures is based on random walks, simple dynamical process that can occur on a network. Random walks can be also used to approximate other types of diffusion processes [46, 47, 28].

3.2.1 Random walk occupation centrality

The random walk occupation centrality [28] of node v is the probability of that node v being visited by a random walker during an infinitely long walk, and it is defined as:

$$C_{rwoc}(v) = \lim_{t \rightarrow \infty} \frac{n_v(t)}{t}, \quad (12)$$

where $n_v(t)$ is the number of times node v is visited by a random walker during time interval t . Different exploration strategies can be used to calculate the occupation centrality, we use the uniform exploration strategy in this paper (i.e. each node jumps to its neighbor with the equal probability). In the weighted networks, jumping probabilities are proportional to the weights of the edges.

The analytical expressions of random walk occupation centrality with a uniform exploration strategy in interconnected multilayer networks are presented in [28].

3.2.2 Random walk betweenness centrality

The most common betweenness is the shortest path betweenness [23, 28], where the centrality of a node v is relative to the number of shortest paths between all pairs of nodes passing through v . However, in real networks, entities (rumors, messages, or internet packets) that travel the network do not always follow the shortest path [48, 49, 28]. Therefore, the random walk betweenness centrality of node v is defined as the amount of random walks between any pair (s, d) of nodes that pass through node v [29].

$$C_{rwbc}(v) = \frac{1}{n_{rwbc}} \sum_{\substack{s, t \in V \\ s \neq t \\ v \neq s, v \neq t}} \mathbf{1}_{v \in \text{Path}_{s \rightarrow t}} \quad (13)$$

Where $n_{rwbc} = 2N(N - 1)$ is the normalization coefficient. The indicator function $\mathbf{1}_{v \in \text{Path}_{s \rightarrow t}}$ is equal to 1 if node v is in the path between nodes s and t , and 0 otherwise. The $\text{Path}_{s \rightarrow t}$ is the random path between nodes s and t in the network. Repeat the random walk process few times to get the different random path. And then we will get the average random walk betweenness centrality.

It will be convenient to get the analytical expression of random walk betweenness centrality of nodes by absorbing random walk. Where the absorbing state is selected to be the destination node d [29, 47]. The extended analytical expression of random walk betweenness centrality for interconnected multilayer networks can be found in [28].

3.2.3 Random walk closeness centrality

A variant of closeness centrality is random walk closeness centrality, the computation of which is based on the mean first-passage time (MFPT). The MFPT is defined as the average number of steps to reach a node d , starting from a given node s . The lower average MFPT indicates that a node is on average more quickly accessible from other nodes. Therefore, a node with a lower average MFPT to all other nodes is considered more “central” in the network. The random walk closeness centrality is defined as the reciprocal of the average MFPT, and it is calculated by the formula:

$$C_{rwcc}(v) = \frac{n - 1}{\sum_{u \in V \setminus \{v\}} \tau_{uv}}, \quad (14)$$

Where τ_{uv} is the MFPT from node u to node v . The MFPT matrix can be calculated analytically by means of Kemeny-Snell fundamental matrix Z [50, 51] or by means of absorbing random walks [47, 52].

The analytical expressions of random walk closeness centrality in interconnected multilayer networks can be found in [28].

3.3 Game-theoretic centrality measures

3.3.1 Shapley value based centrality

The Shapley value is a solution concept in cooperative game theory, which was introduced by Lloyd Shapley in 1953 [31]. It is a measure of the average marginal contribution of a player to all possible coalitions. Shapley value is a unique solution concept in cooperative game theory, it is defined by the formula:

$$\phi(i) = \sum_{S \subseteq N \setminus \{i\}} \frac{|S|!(n - |S| - 1)!}{n!} (v(S \cup \{i\}) - v(S)), \quad (15)$$

Where $S \subseteq V$ represents a coalition, the value of coalition S can be denoted by $v(S)$. We define characteristic function $v(S)$ as half the sum of the weighted degrees of all nodes in the subgraph induced by S as shown in Equation 16.

$$v(S) = \frac{1}{2} \sum_{\{i,j\} \subseteq S} W(i,j) \quad (16)$$

Where $W(i, j)$ is the weight of the edge between nodes i and j within the subgraph induced by S . The factor $\frac{1}{2}$ is used to correct for the fact that in an undirected graph, each edge is counted twice when summing over all node pairs.

The Algorithm 1 describes how to calculate Shapley values based on weighted degree. However, the Shapley value is pretty computationally expensive, especially for large networks because of the number of coalitions³. Therefore, we propose a new approach for calculating Shapley value, we will discuss in the following part.

Algorithm 1 Calculate Shapley Values Based on Weighted Degree

Require: A graph $G(V, E, W)$ with $n = |V|$ nodes

Ensure: Shapley value $\phi(i)$ for each node $i \in V$

```

1: for all nodes  $i \in V$  do
2:   Initialize  $\phi(i) \leftarrow 0$ 
3: end for
4: for all nodes  $i \in V$  do
5:   for all subsets  $S \subseteq V \setminus \{i\}$  do
6:     Compute  $v(S) \leftarrow \sum_{\{j,k\} \subseteq S} W(j,k)$  within subgraph induced by  $S$ 
7:     Compute  $v(S \cup \{i\})$  within subgraph induced by  $S \cup \{i\}$ 
8:      $\Delta v(S, i) \leftarrow v(S \cup \{i\}) - v(S)$ 
9:      $\text{coeff} \leftarrow \frac{|S|!(n - |S| - 1)!}{n!}$ 
10:     $\phi(i) \leftarrow \phi(i) + \text{coeff} \cdot \Delta v(S, i)$ 
11:   end for
12: end for
return  $\phi(i)$  for all  $i \in V$ 

```

3.3.2 Shapley value based centrality approximation

According to the fact that the influence from other nodes will decrease with the increase of path length. We have the following ideas to speed up the calculation:

1. Depth limitation: By limiting the depth of the neighbor considered, the number of subsets that need to be considered is reduced, lowering computational complexity.
2. Local subset iteration: Iterating over subsets only within the local neighbor, rather than the entire graph, decreases the number of iterations.
3. Neighbor size sampling: For larger neighbors, computational complexity is further reduced by random sampling, thereby decreasing the number of subsets iterated over.

Define $\psi(i, d_{max})$ as the set of neighbors of node i up to depth d_{max} , not include node i . We can calculate the Shapley value of node i based on the local neighbor as shown in Equation 17, where $\beta = \frac{\psi(i, d_{max}) + 1}{m + 1}$ is the scaling factor, and m is the maximal neighbors size.

The algorithm for optimized calculation of Shapley values in weighted graphs is shown in Algorithm 2. We use the same characteristic function as in the original Shapley value calculation, but we limit the depth of the neighbor considered and sample subsets from the neighbor to approximate the Shapley value.

³for a network with n nodes, the total number of coalitions are equal to 2^n

$$\phi_a(i) = \begin{cases} \sum_{S \subseteq \psi(i, d_{max})} \frac{v(S \cup \{i\}) - v(S)}{2^{|\psi(i, d_{max})|}} & \text{if } \psi(i, d_{max}) < m, \\ \beta \sum_{S \subseteq \psi(i, d_{max})} \frac{v(S \cup \{i\}) - v(S)}{2^{|\psi(i, d_{max})|}} & \text{if } \psi(i, d_{max}) \geq m. \end{cases} \quad (17)$$

For $\psi(i, d_{max}) \geq m$, we will random sample m neighbors from $\psi(i, d_{max})$ several times and calculate the Shapley value based on the samples. The sampling times $H_{|\psi(i, d_{max})|, m}$ is given by the Formula (18) [53]. Where $\gamma \approx 0.5772156649$ is the Euler-Mascheroni constant. This formula is the mathematical expectation of the number of samples for collecting m neighbors from $\psi(i, d_{max})$ until all neighbors are collected.⁴

$$H_{\psi(i, d_{max}), m} = \left(\frac{\psi(i, d_{max}) + \frac{1}{2}}{m} - \frac{1}{2} \right) (\ln \psi(i, d_{max}) + \gamma) + \frac{1}{2} \quad (18)$$

From the Equation (17), we will get the approximation of the Shapley value, the Shapley value is very close to the real value when the density of the graph not very high (less than 0.7). But in any case, the ratio of each node's approximated Shapley value to the sum of all nodes' approximated Shapley values is very close to the ratio of the real one. Additionally, it's very easy to calculate the Shapley value of the biggest coalition $v(N)$, this makes it possible for us to approximate more accurately. We define the factor ξ as below:

$$\xi = \frac{v(N)}{\sum_{i \in V} \phi_a(i)}$$

We can get the more accurate approximated Shapley value of each node by multiplying the factor ξ with the approximated Shapley value $\phi_a(i)$. We will show the benchmark with this algorithm in the Section 4.2.

3.3.3 Myerson value based centrality

The Myerson value was introduced by Roger Myerson in 1977 [32]. It is a measure of the contribution of participants in a cooperative game that considers the effects of network structure. By modifying the calculation method of the Shapley value, Myerson takes into consideration the connections in the network, thereby reflecting the influence of the network structure on the cooperative game. Consider a game where graph G is a tree, which consists on N nodes and characteristic function is determined by the schema proposed by Jackson [54]; Every direct connection gives to coalition S the impact r , where $0 \leq r \leq 1$. Players also obtain an impact from non-direct connections. This kind of impact will decrease with the increase of the path length. The characteristic function is defined as follows [34]:

$$v(S) = a_1 r + a_2 r^2 + \dots + a_k r^k + \dots + a_L r^L = \sum_{k=1}^L a_k r^k, \quad (19)$$

where L is a maximal distance between two nodes in the coalition; a_k is the number of paths of length k in this coalition; $v(i) = 0, \forall i \in N$.

Mazalov, Trukhina etc. prove that the Equation 20 is a Myerson value for unweighted graphs [55]. where $\sigma_k(i)$ is a number of the paths of the length k which include i . Which can be applied to weighted graph by converting the weight of the edge to the number of paths between two nodes. (i.e. converting a weighted graph to a multigraph) [34]

$$Y_i(v, g) = \frac{\sigma_1(i)}{2} r + \frac{\sigma_2(i)}{3} r^2 + \dots + \frac{\sigma_L(i)}{L+1} r^L = \sum_{k=1}^L \frac{\sigma_k(i)}{k+1} r^k, \quad (20)$$

3.3.4 Myerson value based centrality approximation

However, calculate the Myerson value is also computationally expensive, especially for large networks. Considering the six degrees separation [56], that any two people in the world who don't know each other only need a few intermediaries to establish contact. This means we can reduce the computational expense by limiting the maximal depth L . For a social network, the higher density, the lower intermediate nodes are needed to connect two nodes. We redefine L by the Formula 21, where D is the density of the network:

⁴We can consider this problem as the generalized coupon collector's problem.

Algorithm 2 Optimized Calculation of Shapley Values in Weighted Graphs**Require:** A weighted graph $G = (V, E, W)$, depth limit d_{max} , maximal neighbors size m **Ensure:** Shapley value $\phi_a(i)$ for each node $i \in V$

```

1: Initialize  $\phi(i)_a \leftarrow 0$  for each  $i \in V$ 
2: for  $i \in V$  do
3:    $\psi(i, d_{max}) \leftarrow$  Calculate or retrieve all neighbors of  $i$  up to depth  $d_{max}$ 
4:   if  $|\psi(i, d_{max})| < m$  then
5:     for each subset  $S \subseteq \psi(i, d_{max}) \setminus \{i\}$  do
6:       Compute  $v(S) \leftarrow \sum_{\{j,k\} \subseteq S} W(j,k)$  within subgraph induced by  $S$ 
7:       Compute  $v(S \cup \{i\})$  within subgraph induced by  $S \cup \{i\}$ 
8:        $\Delta v(S, i) \leftarrow v(S \cup \{i\}) - v(S)$ 
9:        $\phi_a(i) \leftarrow \phi_a(i) + \Delta v(S, i)$ 
10:    end for
11:     $\text{coeff} \leftarrow \frac{1}{2^{|\psi(i, d_{max})|}}$ 
12:     $\phi_a(i) \leftarrow \phi_a(i) \cdot \text{coeff}$ , normalize  $\phi_a(i)$  based on the number of subsets
13:  else
14:    Pick up  $m$  neighbors randomly from  $\psi(i, d_{max})$  and repeat  $H_{|\psi(i, d_{max})|, m}$  times
15:    for  $i = 1$  to  $H_{|\psi(i, d_{max})|, m}$  do
16:       $s\_neighbors \leftarrow$  Randomly select a sample of  $m$  neighbors from  $\psi(i, d_{max})$ ,
17:      for each subset  $S \subseteq s\_neighbors \setminus \{i\}$  do
18:        Calculate  $v(S)$  and  $v(S \cup \{i\})$  as before
19:         $\Delta v(S, i) \leftarrow v(S \cup \{i\}) - v(S)$ 
20:         $\phi_a(i) \leftarrow \phi_a(i) + \Delta v(S, i)$ 
21:      end for
22:    end for
23:     $\text{coeff} \leftarrow 1/2^{|\psi(i, d_{max})|} / H_{|\psi(i, d_{max})|, m} \cdot \frac{|\psi(i, d_{max})|+1}{m+1}$ 
24:     $\phi_a(i) \leftarrow \phi_a(i) \cdot \text{coeff}$ 
25:  end if
26: end for
27: Define coefficient  $\xi \leftarrow \frac{v(N)}{\sum_{i \in V} \phi_a(i)}$  ▷ For more accuracy results
28: return  $\phi_a(i) \leftarrow \xi \cdot \phi_a(i)$  for all  $i \in V$ 

```

$$L = \begin{cases} 6 & \text{if } D \leq 0.2, \\ 2 & \text{if } 0.2 < D \leq 0.3, \\ 1 & \text{if } D > 0.3. \end{cases} \quad (21)$$

The algorithm for calculation of Myerson values in weighted graphs is shown in Algorithm 3. We use the same characteristic function as in the Equation 20, but we cutoff the maximal depth to approximate the Myerson value.

Similarly, we can also define the scaling factor ξ for the Myerson value based centrality approximation. The factor ξ is defined as below:

$$\xi = \frac{v(N)}{\sum_{i \in V} Y_i(v, g)}$$

For the $v(N)$ of Myerson value, we need to count the number of paths for all length, i.e. a_1, a_2, \dots, a_L . It's more computationally expensive than the Shapley value. But after the ξ scaling, we will get a more accurate approximation. We will show the comparison in the Section 4.2.

4 Experiments

Network structure has a huge impact on KPIs of opinion dynamics realized on this network. Therefore, we define several characteristics of a network which, in our opinion, have most significant correlation with KPIs of opinion dynamics.

Algorithm 3 Myerson Value for weighted graphs

Require: A weighted graph $G(V, E, W)$, discount factor r (default 0.5), a boolean *weight* for considering edge weights (default True), a boolean *approximate* for approximation (default True), a boolean *scale* for scaling (default False)

Ensure: Myerson value $Y_i(v, g)$ for each node $i \in V$

```

1:  $Y_i(v, g) \leftarrow 0$  for each  $i \in V$  ▷ Initialize Myerson values
2: if approximate then
3:    $L \leftarrow \begin{cases} 1, & \text{if } \text{density}(G) > 0.3 \\ 2, & \text{if } \text{density}(G) > 0.2 \\ 6, & \text{otherwise} \end{cases}$  ▷ Adjust  $L$  based on  $\text{density}(G)$ .
4: else
5:    $L \leftarrow |V| - 1$  ▷ Without approximation
6: end if
7: for all  $i \in V$  do
8:    $l2c \leftarrow$  Initialize a length->count map for paths through  $i$ 
9:   for all pairs  $(start, end)$  in  $V \times V$  do
10:    for all  $path$  in all simple paths from  $start$  to  $end$  with  $length \leq L$  do
11:      if  $node \in path$  then
12:         $length \leftarrow \text{len}(path) - 1$ 
13:        if weight then
14:           $l2c[length] \leftarrow l2c[length] + \min_{(u,v) \in path} w(u, v)$ 
15:        else
16:           $l2c[length] \leftarrow l2c[length] + 1$ 
17:        end if
18:      end if
19:    end for
20:  end for
21:  for all  $(length, count) \in l2c$  do
22:     $count \leftarrow count / 2$  ▷ Correct for double counting
23:     $Y_i(v, g) \leftarrow Y_i(v, g) + \left( count \cdot \frac{r^{length}}{length+1} \right)$ 
24:  end for
25: end for
26: if scale then
27:   Define  $\xi \leftarrow \frac{v(N)}{\sum_{i \in V} Y_i(v, g)}$  ▷ For more accuracy results
28:   return  $Y_i(v, g) \leftarrow \xi \cdot Y_i(v, g)$  for all  $i \in V$ 
29: else
30:   return  $Y_i(v, g)$  for all  $i \in V$ 
31: end if

```

4.1 Centrality experiments description

Due to the computational complexity of the Shapley value and Myerson value, we fixed the number of nodes in the network to 20, and for a given density. We randomly and repeatedly take two different nodes from the graph to add the connection between them until the density reaches the desired value. We designed the following experiments to evaluate the performance of the proposed centrality measures:

1. **Shapley value based centrality:** Density is fixed to 0.1, 0.2, \dots , 1, for each weighted and unweighted graph, we calculate the Shapley value and approximated Shapley value. We compare the results and the calculation time of the two methods.
2. **Myerson value based centrality:** Density is fixed to 0.1, 0.11, \dots , 0.2 (Even a very slight increasing of density will significant increase in computation time.), for each weighted and unweighted graph, we calculate the Myerson value and approximated Myerson value. We compare the results and the calculation time of the two methods. And then we reduce the number of nodes but increase the density to 1 to show the effective of our Myerson value based algorithm.

3. **Comparison with classical centrality measures:** Based on the real social network dataset “Zachary’s karate club”, we generate the two-layer network by adding different internal structures. And simplify the two-layer network to a one-layer weighted network by the method described in Section 2.4. The most important nodes in the network are node 0 (instructor — Mr Hi) and node 33 (manager — John A). We define the accuracy of the centrality measures as shown in Equation 22. We compare the accuracy of the proposed centrality measures with the classical centrality measures (betweenness and closeness centralities).

$$\text{Accuracy} = \frac{|\text{Top 2 nodes of the proposed centrality measures} \cap \{0, 33\}|}{2} \quad (22)$$

4.2 Centrality experiments results

Table 1 shows the comparison results of the Shapley value based approach, where “SV” refers to “Shapley value”, “ASV” refers to “Approximated Shapley value” and “RMSE” refers to the root mean square error. The lower RMSE indicates the more accurate approximation. The “Ratio” is the ratio of the (approximated) Shapley value of each node to the sum of all nodes’ (approximated) Shapley values. The “RMSE Ratio” is the ratio of the RMSE of the approximated Shapley value to the RMSE of the Shapley value. The “Weighted” column indicates whether the edge weight is considered in the calculation.

The calculation time is much faster (see the columns “SV Time” and “ASV Time”) than the original Shapley value calculation. And the RMSE of the approximated Shapley value is very low, the RMSE ratio is also very low for both weighted and unweighted graphs.

Table 1: Shapley value results with ξ scaling factor

| Graph | SV Time | ASV Time | RMSE ASV | RMSE Ratio ASV | Weighted |
|--------|------------------|---------------------|----------------------|----------------------|----------|
| 20-0.1 | $7.2 \cdot 10^2$ | $2.2 \cdot 10^{-3}$ | $2.6 \cdot 10^{-22}$ | $5.5 \cdot 10^{-27}$ | True |
| 20-0.2 | $8.7 \cdot 10^2$ | $1.9 \cdot 10^{-2}$ | $3.1 \cdot 10^{-22}$ | $5.6 \cdot 10^{-27}$ | True |
| 20-0.3 | $1 \cdot 10^3$ | $1.5 \cdot 10^{-1}$ | $1.6 \cdot 10^{-22}$ | $1.2 \cdot 10^{-27}$ | True |
| 20-0.4 | $1.2 \cdot 10^3$ | $9.3 \cdot 10^{-1}$ | $1.7 \cdot 10^{-22}$ | $6.1 \cdot 10^{-28}$ | True |
| 20-0.5 | $1.3 \cdot 10^3$ | $2.2 \cdot 10^0$ | $7.1 \cdot 10^{-23}$ | $2 \cdot 10^{-28}$ | True |
| 20-0.6 | $1.5 \cdot 10^3$ | $1.9 \cdot 10^1$ | $7.7 \cdot 10^{-23}$ | $1.8 \cdot 10^{-28}$ | True |
| 20-0.7 | $1.6 \cdot 10^3$ | $4.7 \cdot 10^1$ | $3.3 \cdot 10^{-2}$ | $6 \cdot 10^{-8}$ | True |
| 20-0.8 | $1.7 \cdot 10^3$ | $1.7 \cdot 10^2$ | $2 \cdot 10^0$ | $2.9 \cdot 10^{-6}$ | True |
| 20-0.9 | $1.8 \cdot 10^3$ | $2.5 \cdot 10^2$ | $6.9 \cdot 10^0$ | $7.9 \cdot 10^{-6}$ | True |
| 20-1.0 | $1.9 \cdot 10^3$ | $3.2 \cdot 10^2$ | $9.9 \cdot 10^0$ | $9 \cdot 10^{-6}$ | True |
| 20-0.1 | $7.2 \cdot 10^2$ | $3.4 \cdot 10^{-3}$ | $4.5 \cdot 10^{-23}$ | $1.1 \cdot 10^{-26}$ | False |
| 20-0.2 | $8.8 \cdot 10^2$ | $1.6 \cdot 10^{-2}$ | $1.1 \cdot 10^{-22}$ | $7.8 \cdot 10^{-27}$ | False |
| 20-0.3 | $1 \cdot 10^3$ | $9.6 \cdot 10^{-2}$ | $1.1 \cdot 10^{-22}$ | $6.6 \cdot 10^{-27}$ | False |
| 20-0.4 | $1.2 \cdot 10^3$ | $5.5 \cdot 10^{-1}$ | $1.5 \cdot 10^{-22}$ | $1.6 \cdot 10^{-26}$ | False |
| 20-0.5 | $1.3 \cdot 10^3$ | $2.9 \cdot 10^0$ | $1.1 \cdot 10^{-22}$ | $8.6 \cdot 10^{-27}$ | False |
| 20-0.6 | $1.5 \cdot 10^3$ | $2.5 \cdot 10^1$ | $1.4 \cdot 10^{-22}$ | $9.4 \cdot 10^{-27}$ | False |
| 20-0.7 | $1.6 \cdot 10^3$ | $6.2 \cdot 10^1$ | $3.8 \cdot 10^{-4}$ | $2.1 \cdot 10^{-8}$ | False |
| 20-0.8 | $1.7 \cdot 10^3$ | $1.7 \cdot 10^2$ | $1.8 \cdot 10^{-3}$ | $7.7 \cdot 10^{-8}$ | False |
| 20-0.9 | $1.8 \cdot 10^3$ | $2.5 \cdot 10^2$ | $2 \cdot 10^{-3}$ | $6.9 \cdot 10^{-8}$ | False |
| 20-1.0 | $1.9 \cdot 10^3$ | $3.2 \cdot 10^2$ | $4.1 \cdot 10^{-21}$ | $8.6 \cdot 10^{-34}$ | False |

Table 3 shows the comparison results of the Myerson value based approach with scaling factor ξ . From the “MV Time” and “AMV Time”, we can see the computational complexity of Myerson value based centrality grows rapidly with the increase of the density of the network.

The RMSE of the approximated Myerson value grows with the increase of the density of the network, but the RMSE ratio is very low. Therefore, we can use the approximation of Myerson value as the centrality for nodes in the network. Table 2 shows the comparison results of the Myerson value based approach without scaling factor ξ . By comparing “AMV Time” in Table 2 and Table 3, we can see without ξ the calculation time is much faster.

To show the effective of our algorithm for Myerson value even in the high density graph, we reduce the number of node to 10, and increase the density from 0.05 to 1 with step 0.05. The results are shown in Table 4 and Table 5.

By comparing the pair of Table 2, Table 3 and Table 4, Table 5, we can get the conclusion that the scaling factor ξ has a very limited effect on reducing the error of approximation Myerson value and ξ increase the computation time a lot. But the error of ratio is very small. **Therefore We recommend to use the Myerson value based centrality approximation without the scaling factor ξ and use the ratio as the approximation of the Myerson value.**

Table 2: Myerson value results without ξ scaling

| Graph | MV Time | AMV Time | RMSE AMV | RMSE Ratio AMV | Weighted |
|---------|----------------------|----------------------|----------------------|----------------------|----------|
| 20-0.1 | $1.03 \cdot 10^{-1}$ | $1.62 \cdot 10^{-1}$ | $4.37 \cdot 10^{-4}$ | $1.48 \cdot 10^{-8}$ | True |
| 20-0.11 | $1.91 \cdot 10^{-1}$ | $1.67 \cdot 10^{-1}$ | $8.75 \cdot 10^{-4}$ | $1.7 \cdot 10^{-8}$ | True |
| 20-0.12 | $4.17 \cdot 10^{-1}$ | $2.23 \cdot 10^{-1}$ | $1.54 \cdot 10^{-1}$ | $5.28 \cdot 10^{-7}$ | True |
| 20-0.13 | $1.02 \cdot 10^0$ | $3.56 \cdot 10^{-1}$ | $5.28 \cdot 10^{-1}$ | $8.15 \cdot 10^{-7}$ | True |
| 20-0.14 | $2.21 \cdot 10^0$ | $6.15 \cdot 10^{-1}$ | $2.14 \cdot 10^0$ | $1.93 \cdot 10^{-6}$ | True |
| 20-0.15 | $8.78 \cdot 10^0$ | $9.24 \cdot 10^{-1}$ | $1.89 \cdot 10^1$ | $4.3 \cdot 10^{-6}$ | True |
| 20-0.16 | $1.8 \cdot 10^1$ | $1.48 \cdot 10^0$ | $1.27 \cdot 10^2$ | $1.25 \cdot 10^{-5}$ | True |
| 20-0.17 | $2.87 \cdot 10^1$ | $2.14 \cdot 10^0$ | $4.06 \cdot 10^2$ | $3.24 \cdot 10^{-5}$ | True |
| 20-0.18 | $6.34 \cdot 10^1$ | $2.77 \cdot 10^0$ | $1.55 \cdot 10^3$ | $4.7 \cdot 10^{-5}$ | True |
| 20-0.19 | $1.45 \cdot 10^2$ | $3.58 \cdot 10^0$ | $4.82 \cdot 10^3$ | $8.66 \cdot 10^{-5}$ | True |
| 20-0.2 | $2.94 \cdot 10^2$ | $4.45 \cdot 10^0$ | $1.33 \cdot 10^4$ | $1.35 \cdot 10^{-4}$ | True |
| 20-0.1 | $3.3 \cdot 10^{-1}$ | $1.96 \cdot 10^{-1}$ | $1.12 \cdot 10^{-2}$ | $1.43 \cdot 10^{-6}$ | False |
| 20-0.11 | $3.45 \cdot 10^{-1}$ | $2.16 \cdot 10^{-1}$ | $1.73 \cdot 10^{-2}$ | $1.41 \cdot 10^{-6}$ | False |
| 20-0.12 | $4.87 \cdot 10^{-1}$ | $2.17 \cdot 10^{-1}$ | $3.43 \cdot 10^{-2}$ | $1.52 \cdot 10^{-6}$ | False |
| 20-0.13 | $1.37 \cdot 10^0$ | $3.79 \cdot 10^{-1}$ | $3.95 \cdot 10^{-1}$ | $5.73 \cdot 10^{-6}$ | False |
| 20-0.14 | $3.69 \cdot 10^0$ | $5.81 \cdot 10^{-1}$ | $2.71 \cdot 10^0$ | $1.53 \cdot 10^{-5}$ | False |
| 20-0.15 | $7.65 \cdot 10^0$ | $1.05 \cdot 10^0$ | $1.38 \cdot 10^1$ | $2.75 \cdot 10^{-5}$ | False |
| 20-0.16 | $1.71 \cdot 10^1$ | $1.38 \cdot 10^0$ | $5.94 \cdot 10^1$ | $4.19 \cdot 10^{-5}$ | False |
| 20-0.17 | $4.28 \cdot 10^1$ | $1.62 \cdot 10^0$ | $2.97 \cdot 10^2$ | $6.29 \cdot 10^{-5}$ | False |
| 20-0.18 | $8.25 \cdot 10^1$ | $1.88 \cdot 10^0$ | $8.04 \cdot 10^2$ | $6.73 \cdot 10^{-5}$ | False |
| 20-0.19 | $1.69 \cdot 10^2$ | $2.56 \cdot 10^0$ | $2.72 \cdot 10^3$ | $7.6 \cdot 10^{-5}$ | False |
| 20-0.2 | $3.66 \cdot 10^2$ | $3.57 \cdot 10^0$ | $8.75 \cdot 10^3$ | $1.31 \cdot 10^{-4}$ | False |

Table 3: Myerson value results with ξ scaling

| Graph | MV Time | AMV Time | RMSE AMV | RMSE Ratio AMV | Weighted |
|---------|----------------------|----------------------|----------------------|----------------------|----------|
| 20-0.1 | $1.23 \cdot 10^{-1}$ | $1.1 \cdot 10^{-1}$ | $1.98 \cdot 10^{-4}$ | $1.48 \cdot 10^{-8}$ | True |
| 20-0.11 | $1.57 \cdot 10^{-1}$ | $2.11 \cdot 10^{-1}$ | $3.21 \cdot 10^{-4}$ | $1.7 \cdot 10^{-8}$ | True |
| 20-0.12 | $4.53 \cdot 10^{-1}$ | $2.21 \cdot 10^{-1}$ | $1.55 \cdot 10^{-2}$ | $5.28 \cdot 10^{-7}$ | True |
| 20-0.13 | $9.1 \cdot 10^{-1}$ | $4.33 \cdot 10^{-1}$ | $3.15 \cdot 10^{-2}$ | $8.15 \cdot 10^{-7}$ | True |
| 20-0.14 | $2.09 \cdot 10^0$ | $6.7 \cdot 10^{-1}$ | $1.08 \cdot 10^{-1}$ | $1.93 \cdot 10^{-6}$ | True |
| 20-0.15 | $7.83 \cdot 10^0$ | $1.24 \cdot 10^0$ | $4.81 \cdot 10^{-1}$ | $4.3 \cdot 10^{-6}$ | True |
| 20-0.16 | $1.65 \cdot 10^1$ | $2.24 \cdot 10^0$ | $3.85 \cdot 10^0$ | $1.25 \cdot 10^{-5}$ | True |
| 20-0.17 | $2.63 \cdot 10^1$ | $3.28 \cdot 10^0$ | $2.36 \cdot 10^1$ | $3.24 \cdot 10^{-5}$ | True |
| 20-0.18 | $5.91 \cdot 10^1$ | $5.91 \cdot 10^0$ | $6.15 \cdot 10^1$ | $4.7 \cdot 10^{-5}$ | True |
| 20-0.19 | $1.41 \cdot 10^2$ | $1.15 \cdot 10^1$ | $2.07 \cdot 10^2$ | $8.66 \cdot 10^{-5}$ | True |
| 20-0.2 | $2.92 \cdot 10^2$ | $2.06 \cdot 10^1$ | $6.48 \cdot 10^2$ | $1.35 \cdot 10^{-4}$ | True |
| 20-0.1 | $2.75 \cdot 10^{-1}$ | $2.43 \cdot 10^{-1}$ | $1.59 \cdot 10^{-3}$ | $1.43 \cdot 10^{-6}$ | False |
| 20-0.11 | $3.64 \cdot 10^{-1}$ | $1.94 \cdot 10^{-1}$ | $1.81 \cdot 10^{-3}$ | $1.41 \cdot 10^{-6}$ | False |
| 20-0.12 | $4.56 \cdot 10^{-1}$ | $2.47 \cdot 10^{-1}$ | $2.65 \cdot 10^{-3}$ | $1.52 \cdot 10^{-6}$ | False |
| 20-0.13 | $1.34 \cdot 10^0$ | $4.13 \cdot 10^{-1}$ | $2.01 \cdot 10^{-2}$ | $5.73 \cdot 10^{-6}$ | False |
| 20-0.14 | $3.33 \cdot 10^0$ | $6.97 \cdot 10^{-1}$ | $1.18 \cdot 10^{-1}$ | $1.53 \cdot 10^{-5}$ | False |
| 20-0.15 | $7.17 \cdot 10^0$ | $1.29 \cdot 10^0$ | $5.64 \cdot 10^{-1}$ | $2.75 \cdot 10^{-5}$ | False |
| 20-0.16 | $1.55 \cdot 10^1$ | $2.01 \cdot 10^0$ | $1.92 \cdot 10^0$ | $4.19 \cdot 10^{-5}$ | False |
| 20-0.17 | $3.93 \cdot 10^1$ | $3.3 \cdot 10^0$ | $7.44 \cdot 10^0$ | $6.29 \cdot 10^{-5}$ | False |
| 20-0.18 | $7.78 \cdot 10^1$ | $5.58 \cdot 10^0$ | $1.6 \cdot 10^1$ | $6.73 \cdot 10^{-5}$ | False |
| 20-0.19 | $1.64 \cdot 10^2$ | $1.06 \cdot 10^1$ | $4.58 \cdot 10^1$ | $7.6 \cdot 10^{-5}$ | False |
| 20-0.2 | $3.43 \cdot 10^2$ | $1.99 \cdot 10^1$ | $2.06 \cdot 10^2$ | $1.31 \cdot 10^{-4}$ | False |

Table 4: Myerson value results without ξ scaling in 10-node network

| Graph | MV Time | AMV Time | RMSE AMV | RMSE Ratio AMV | Weighted |
|---------|----------------------|----------------------|----------------------|-----------------------|----------|
| 10-0.05 | $1.24 \cdot 10^{-3}$ | $1.59 \cdot 10^{-2}$ | $0 \cdot 10^0$ | $0 \cdot 10^0$ | True |
| 10-0.1 | $1.79 \cdot 10^{-3}$ | $1.58 \cdot 10^{-3}$ | $0 \cdot 10^0$ | $0 \cdot 10^0$ | True |
| 10-0.15 | $1.27 \cdot 10^{-2}$ | $3.17 \cdot 10^{-3}$ | $0 \cdot 10^0$ | $0 \cdot 10^0$ | True |
| 10-0.2 | $7.33 \cdot 10^{-3}$ | $1.05 \cdot 10^{-2}$ | $9.65 \cdot 10^{-6}$ | $7.63 \cdot 10^{-10}$ | True |
| 10-0.25 | $1.49 \cdot 10^{-2}$ | $2.89 \cdot 10^{-3}$ | $3.27 \cdot 10^1$ | $1.64 \cdot 10^{-4}$ | True |
| 10-0.3 | $6.69 \cdot 10^{-2}$ | $3.35 \cdot 10^{-3}$ | $2.79 \cdot 10^2$ | $1.91 \cdot 10^{-4}$ | True |
| 10-0.35 | $1.17 \cdot 10^{-1}$ | $1.78 \cdot 10^{-3}$ | $1.85 \cdot 10^3$ | $5.12 \cdot 10^{-4}$ | True |
| 10-0.4 | $2.6 \cdot 10^{-1}$ | $1.2 \cdot 10^{-3}$ | $4.58 \cdot 10^3$ | $4.08 \cdot 10^{-4}$ | True |
| 10-0.45 | $5.53 \cdot 10^{-1}$ | $1.21 \cdot 10^{-3}$ | $1.05 \cdot 10^4$ | $6.26 \cdot 10^{-4}$ | True |
| 10-0.5 | $1.21 \cdot 10^0$ | $1.37 \cdot 10^{-3}$ | $1.56 \cdot 10^4$ | $5.53 \cdot 10^{-4}$ | True |
| 10-0.55 | $2.56 \cdot 10^0$ | $1.26 \cdot 10^{-3}$ | $3.92 \cdot 10^4$ | $4.49 \cdot 10^{-4}$ | True |
| 10-0.6 | $5.7 \cdot 10^0$ | $1.62 \cdot 10^{-3}$ | $1.11 \cdot 10^5$ | $6.17 \cdot 10^{-4}$ | True |
| 10-0.65 | $1.05 \cdot 10^1$ | $1.33 \cdot 10^{-3}$ | $2.31 \cdot 10^5$ | $7.47 \cdot 10^{-4}$ | True |
| 10-0.7 | $1.99 \cdot 10^1$ | $1.33 \cdot 10^{-3}$ | $5.19 \cdot 10^5$ | $6.84 \cdot 10^{-4}$ | True |
| 10-0.75 | $3.55 \cdot 10^1$ | $6.44 \cdot 10^{-3}$ | $1 \cdot 10^6$ | $5.96 \cdot 10^{-4}$ | True |
| 10-0.8 | $7.36 \cdot 10^1$ | $1.38 \cdot 10^{-3}$ | $3.42 \cdot 10^6$ | $5.9 \cdot 10^{-4}$ | True |
| 10-0.85 | $1.15 \cdot 10^2$ | $1.38 \cdot 10^{-3}$ | $8.11 \cdot 10^6$ | $3.76 \cdot 10^{-4}$ | True |
| 10-0.9 | $1.73 \cdot 10^2$ | $1.39 \cdot 10^{-3}$ | $1.63 \cdot 10^7$ | $3.92 \cdot 10^{-4}$ | True |
| 10-0.95 | $2.48 \cdot 10^2$ | $1.37 \cdot 10^{-3}$ | $2.74 \cdot 10^7$ | $3.7 \cdot 10^{-4}$ | True |
| 10-1.0 | $4.33 \cdot 10^2$ | $1.37 \cdot 10^{-3}$ | $7.31 \cdot 10^7$ | $2.79 \cdot 10^{-4}$ | True |
| 10-0.05 | $1.15 \cdot 10^{-3}$ | $1.06 \cdot 10^{-3}$ | $0 \cdot 10^0$ | $0 \cdot 10^0$ | False |
| 10-0.1 | $2.09 \cdot 10^{-3}$ | $1.99 \cdot 10^{-3}$ | $0 \cdot 10^0$ | $0 \cdot 10^0$ | False |
| 10-0.15 | $3.4 \cdot 10^{-3}$ | $2.84 \cdot 10^{-3}$ | $0 \cdot 10^0$ | $0 \cdot 10^0$ | False |
| 10-0.2 | $7.57 \cdot 10^{-3}$ | $1.08 \cdot 10^{-2}$ | $0 \cdot 10^0$ | $0 \cdot 10^0$ | False |
| 10-0.25 | $3.14 \cdot 10^{-2}$ | $8.37 \cdot 10^{-3}$ | $2.56 \cdot 10^0$ | $1.57 \cdot 10^{-4}$ | False |
| 10-0.3 | $3.12 \cdot 10^{-2}$ | $3.11 \cdot 10^{-3}$ | $8.85 \cdot 10^0$ | $9.04 \cdot 10^{-5}$ | False |
| 10-0.35 | $8.49 \cdot 10^{-2}$ | $1.13 \cdot 10^{-3}$ | $5.98 \cdot 10^1$ | $1.53 \cdot 10^{-4}$ | False |
| 10-0.4 | $2.18 \cdot 10^{-1}$ | $1.33 \cdot 10^{-3}$ | $2.28 \cdot 10^2$ | $1.29 \cdot 10^{-4}$ | False |
| 10-0.45 | $4.74 \cdot 10^{-1}$ | $1.16 \cdot 10^{-3}$ | $6.23 \cdot 10^2$ | $9.58 \cdot 10^{-5}$ | False |
| 10-0.5 | $9.61 \cdot 10^{-1}$ | $1.17 \cdot 10^{-3}$ | $1.81 \cdot 10^3$ | $8.71 \cdot 10^{-5}$ | False |
| 10-0.55 | $1.95 \cdot 10^0$ | $1.21 \cdot 10^{-3}$ | $4.91 \cdot 10^3$ | $7.4 \cdot 10^{-5}$ | False |
| 10-0.6 | $4.15 \cdot 10^0$ | $1.3 \cdot 10^{-3}$ | $1.97 \cdot 10^4$ | $4.98 \cdot 10^{-5}$ | False |
| 10-0.65 | $7.11 \cdot 10^0$ | $1.24 \cdot 10^{-3}$ | $4.79 \cdot 10^4$ | $5.33 \cdot 10^{-5}$ | False |
| 10-0.7 | $1.14 \cdot 10^1$ | $1.33 \cdot 10^{-3}$ | $1.07 \cdot 10^5$ | $9.37 \cdot 10^{-5}$ | False |
| 10-0.75 | $1.86 \cdot 10^1$ | $3.51 \cdot 10^{-3}$ | $2.46 \cdot 10^5$ | $1.6 \cdot 10^{-4}$ | False |
| 10-0.8 | $3.77 \cdot 10^1$ | $1.39 \cdot 10^{-3}$ | $8.53 \cdot 10^5$ | $1.07 \cdot 10^{-4}$ | False |
| 10-0.85 | $5.26 \cdot 10^1$ | $1.29 \cdot 10^{-3}$ | $1.73 \cdot 10^6$ | $1.35 \cdot 10^{-4}$ | False |
| 10-0.9 | $7.45 \cdot 10^1$ | $1.31 \cdot 10^{-3}$ | $3.64 \cdot 10^6$ | $9.85 \cdot 10^{-5}$ | False |
| 10-0.95 | $1.05 \cdot 10^2$ | $1.3 \cdot 10^{-3}$ | $7.74 \cdot 10^6$ | $4.85 \cdot 10^{-5}$ | False |
| 10-1.0 | $1.71 \cdot 10^2$ | $1.28 \cdot 10^{-3}$ | $2.16 \cdot 10^7$ | $0 \cdot 10^0$ | False |

From Table 1, we see the weighted graph with density 1.0 has the highest RMSE. And the weighted graph with density 0.2 in Table 3 has the highest RMSE. Table 6 and Table 7 show the comparison of the real value and approximated value for each node with the relative error.

From Table 6, we can say even for the biggest RMSE, our algorithm provide a very accurate approximation for Shapley value.

From Table 7, we can see some nodes have a high relative error but some nodes are not. The reason is that in the approximation we count the number of paths not for all lengths ($length \leq L$). We can increase the L to make the more accurate result, but it will increase the computational complexity.

Table 8 shows the comparison with classical centrality measures. Both proposed centrality measures have a higher accuracy than the classical centrality measures. Especially, the Shapley value based centrality can identify the most important nodes with 100% accuracy. For the Myerson value based centrality, it has 50% accuracy for the special case (karate-twoStar-34), because the Node 17 another center node in the internal layer. For the betweenness centrality, it work not well for the high-density network. Closeness centrality has a worst accuracy in this case.

Table 5: Myerson value results with ξ scaling in 10-node network

| Graph | MV Time | AMV Time | RMSE AMV | RMSE Ratio AMV | Weighted |
|---------|----------------------|----------------------|-----------------------|-----------------------|----------|
| 10-0.05 | $1.24 \cdot 10^{-3}$ | $1.22 \cdot 10^{-3}$ | $0 \cdot 10^0$ | $0 \cdot 10^0$ | True |
| 10-0.1 | $3.08 \cdot 10^{-3}$ | $1.99 \cdot 10^{-3}$ | $6.24 \cdot 10^{-32}$ | $0 \cdot 10^0$ | True |
| 10-0.15 | $4.67 \cdot 10^{-3}$ | $3.73 \cdot 10^{-3}$ | $0 \cdot 10^0$ | $0 \cdot 10^0$ | True |
| 10-0.2 | $1.2 \cdot 10^{-2}$ | $1.74 \cdot 10^{-2}$ | $3.25 \cdot 10^{-6}$ | $7.63 \cdot 10^{-10}$ | True |
| 10-0.25 | $1.46 \cdot 10^{-2}$ | $4.48 \cdot 10^{-3}$ | $1.67 \cdot 10^0$ | $1.64 \cdot 10^{-4}$ | True |
| 10-0.3 | $4.97 \cdot 10^{-2}$ | $8.24 \cdot 10^{-3}$ | $6.05 \cdot 10^0$ | $1.91 \cdot 10^{-4}$ | True |
| 10-0.35 | $1.05 \cdot 10^{-1}$ | $1.69 \cdot 10^{-2}$ | $3.5 \cdot 10^1$ | $5.12 \cdot 10^{-4}$ | True |
| 10-0.4 | $2.57 \cdot 10^{-1}$ | $2.63 \cdot 10^{-2}$ | $6.41 \cdot 10^1$ | $4.08 \cdot 10^{-4}$ | True |
| 10-0.45 | $5.52 \cdot 10^{-1}$ | $7.07 \cdot 10^{-2}$ | $2.14 \cdot 10^2$ | $6.26 \cdot 10^{-4}$ | True |
| 10-0.5 | $1.18 \cdot 10^0$ | $1.27 \cdot 10^{-1}$ | $2.91 \cdot 10^2$ | $5.53 \cdot 10^{-4}$ | True |
| 10-0.55 | $2.5 \cdot 10^0$ | $3.8 \cdot 10^{-1}$ | $5.78 \cdot 10^2$ | $4.49 \cdot 10^{-4}$ | True |
| 10-0.6 | $5.81 \cdot 10^0$ | $5.76 \cdot 10^{-1}$ | $2.15 \cdot 10^3$ | $6.17 \cdot 10^{-4}$ | True |
| 10-0.65 | $1.06 \cdot 10^1$ | $1.24 \cdot 10^0$ | $5.36 \cdot 10^3$ | $7.47 \cdot 10^{-4}$ | True |
| 10-0.7 | $1.98 \cdot 10^1$ | $2.14 \cdot 10^0$ | $1.12 \cdot 10^4$ | $6.84 \cdot 10^{-4}$ | True |
| 10-0.75 | $3.57 \cdot 10^1$ | $3.66 \cdot 10^0$ | $1.9 \cdot 10^4$ | $5.96 \cdot 10^{-4}$ | True |
| 10-0.8 | $7.43 \cdot 10^1$ | $6.77 \cdot 10^0$ | $6.41 \cdot 10^4$ | $5.9 \cdot 10^{-4}$ | True |
| 10-0.85 | $1.16 \cdot 10^2$ | $1.11 \cdot 10^1$ | $9.71 \cdot 10^4$ | $3.76 \cdot 10^{-4}$ | True |
| 10-0.9 | $1.75 \cdot 10^2$ | $1.71 \cdot 10^1$ | $2.03 \cdot 10^5$ | $3.92 \cdot 10^{-4}$ | True |
| 10-0.95 | $2.48 \cdot 10^2$ | $2.45 \cdot 10^1$ | $3.22 \cdot 10^5$ | $3.7 \cdot 10^{-4}$ | True |
| 10-1.0 | $4.33 \cdot 10^2$ | $4.33 \cdot 10^1$ | $6.49 \cdot 10^5$ | $2.79 \cdot 10^{-4}$ | True |
| 10-0.05 | $1.23 \cdot 10^{-3}$ | $1.29 \cdot 10^{-3}$ | $0 \cdot 10^0$ | $0 \cdot 10^0$ | False |
| 10-0.1 | $2.28 \cdot 10^{-3}$ | $2.55 \cdot 10^{-3}$ | $0 \cdot 10^0$ | $0 \cdot 10^0$ | False |
| 10-0.15 | $4.91 \cdot 10^{-3}$ | $1.73 \cdot 10^{-2}$ | $0 \cdot 10^0$ | $0 \cdot 10^0$ | False |
| 10-0.2 | $2.15 \cdot 10^{-2}$ | $7.96 \cdot 10^{-3}$ | $2.16 \cdot 10^{-31}$ | $2.65 \cdot 10^{-33}$ | False |
| 10-0.25 | $1.64 \cdot 10^{-2}$ | $9.18 \cdot 10^{-3}$ | $5.35 \cdot 10^{-2}$ | $1.57 \cdot 10^{-4}$ | False |
| 10-0.3 | $4.56 \cdot 10^{-2}$ | $6.48 \cdot 10^{-3}$ | $7.23 \cdot 10^{-2}$ | $9.04 \cdot 10^{-5}$ | False |
| 10-0.35 | $6.45 \cdot 10^{-2}$ | $6.84 \cdot 10^{-3}$ | $3.23 \cdot 10^{-1}$ | $1.53 \cdot 10^{-4}$ | False |
| 10-0.4 | $2.43 \cdot 10^{-1}$ | $1.99 \cdot 10^{-2}$ | $1.02 \cdot 10^0$ | $1.29 \cdot 10^{-4}$ | False |
| 10-0.45 | $4.54 \cdot 10^{-1}$ | $3.73 \cdot 10^{-2}$ | $2 \cdot 10^0$ | $9.58 \cdot 10^{-5}$ | False |
| 10-0.5 | $9.12 \cdot 10^{-1}$ | $8.23 \cdot 10^{-2}$ | $5.1 \cdot 10^0$ | $8.71 \cdot 10^{-5}$ | False |
| 10-0.55 | $1.86 \cdot 10^0$ | $2.11 \cdot 10^{-1}$ | $1.15 \cdot 10^1$ | $7.4 \cdot 10^{-5}$ | False |
| 10-0.6 | $4.29 \cdot 10^0$ | $3.61 \cdot 10^{-1}$ | $3.03 \cdot 10^1$ | $4.98 \cdot 10^{-5}$ | False |
| 10-0.65 | $7.36 \cdot 10^0$ | $6.8 \cdot 10^{-1}$ | $7.83 \cdot 10^1$ | $5.33 \cdot 10^{-5}$ | False |
| 10-0.7 | $1.14 \cdot 10^1$ | $1.51 \cdot 10^0$ | $3.05 \cdot 10^2$ | $9.37 \cdot 10^{-5}$ | False |
| 10-0.75 | $1.94 \cdot 10^1$ | $2.03 \cdot 10^0$ | $1.23 \cdot 10^3$ | $1.6 \cdot 10^{-4}$ | False |
| 10-0.8 | $3.74 \cdot 10^1$ | $3.41 \cdot 10^0$ | $2.9 \cdot 10^3$ | $1.07 \cdot 10^{-4}$ | False |
| 10-0.85 | $5.27 \cdot 10^1$ | $5.04 \cdot 10^0$ | $7.35 \cdot 10^3$ | $1.35 \cdot 10^{-4}$ | False |
| 10-0.9 | $7.45 \cdot 10^1$ | $6.5 \cdot 10^0$ | $1.13 \cdot 10^4$ | $9.85 \cdot 10^{-5}$ | False |
| 10-0.95 | $1.05 \cdot 10^2$ | $9.53 \cdot 10^0$ | $1.19 \cdot 10^4$ | $4.85 \cdot 10^{-5}$ | False |
| 10-1.0 | $1.71 \cdot 10^2$ | $1.63 \cdot 10^1$ | $0 \cdot 10^0$ | $0 \cdot 10^0$ | False |

Table 6: Real Shapley value vs approximated Shapley value for “graph-1.0”

| Nodes | SV | SV ratio | ASV | ASV ratio | Rel. Error ASV/SV |
|-------|---------|----------|---------|-----------|------------------------|
| 0 | 52.0000 | 4.96% | 53.3579 | 5.09% | 2.61% |
| 1 | 46.5000 | 4.43% | 46.5090 | 4.43% | $1.83 \cdot 10^{-2}\%$ |
| 2 | 50.5000 | 4.81% | 49.0574 | 4.68% | -2.86% |
| 3 | 53.0000 | 5.05% | 53.6764 | 5.12% | 1.28% |
| 4 | 50.5000 | 4.81% | 50.0131 | 4.77% | -0.96% |
| 5 | 50.0000 | 4.77% | 54.3135 | 5.18% | 8.63% |
| 6 | 50.0000 | 4.77% | 51.2873 | 4.89% | 2.57% |
| 7 | 63.0000 | 6.01% | 62.5960 | 5.97% | -0.64% |
| 8 | 55.0000 | 5.24% | 53.3579 | 5.09% | -2.98% |
| 9 | 44.0000 | 4.19% | 44.4384 | 4.24% | 0.99% |
| 10 | 49.5000 | 4.72% | 50.3316 | 4.80% | 1.68% |
| 11 | 51.0000 | 4.86% | 51.6058 | 4.92% | 1.19% |
| 12 | 64.0000 | 6.10% | 62.9145 | 6.00% | -1.70% |
| 13 | 49.0000 | 4.67% | 49.0574 | 4.68% | 0.12% |
| 14 | 48.0000 | 4.58% | 47.9425 | 4.57% | -0.12% |
| 15 | 63.5000 | 6.05% | 63.0738 | 6.01% | -0.67% |
| 16 | 54.0000 | 5.15% | 54.4728 | 5.19% | 0.87% |
| 17 | 57.0000 | 5.43% | 57.0213 | 5.44% | $3.66 \cdot 10^{-2}\%$ |
| 18 | 53.0000 | 5.05% | 52.0837 | 4.97% | -1.73% |
| 19 | 45.5000 | 4.34% | 41.8899 | 3.99% | -7.93% |

Table 7: Real Myerson value vs approximated Myerson value for “graph-0.2”

| Nodes | MV | MV ratio | AMV | AMV ratio | Rel. Error AMV/MV |
|-------|----------|----------|----------|-----------|-------------------|
| 0 | 143.2672 | 6.53% | 144.0222 | 6.56% | 0.53% |
| 1 | 68.7002 | 3.13% | 49.3370 | 2.25% | −28.18% |
| 2 | 68.0767 | 3.10% | 81.6335 | 3.72% | 19.91% |
| 3 | 104.6799 | 4.77% | 109.9763 | 5.01% | 5.06% |
| 4 | 164.0880 | 7.48% | 157.1853 | 7.16% | −4.21% |
| 5 | 114.6388 | 5.22% | 106.1499 | 4.84% | −7.40% |
| 6 | 16.7705 | 0.76% | 17.8578 | 0.81% | 6.48% |
| 7 | 228.8444 | 10.43% | 251.4307 | 11.46% | 9.87% |
| 8 | 33.7682 | 1.54% | 24.3128 | 1.11% | −28.00% |
| 9 | 36.1832 | 1.65% | 28.1827 | 1.28% | −22.11% |
| 10 | 184.1740 | 8.39% | 192.6532 | 8.78% | 4.60% |
| 11 | 79.7901 | 3.64% | 69.8602 | 3.18% | −12.45% |
| 12 | 56.7906 | 2.59% | 53.0066 | 2.42% | −6.66% |
| 13 | 48.8678 | 2.23% | 46.0495 | 2.10% | −5.77% |
| 14 | 107.3196 | 4.89% | 93.9069 | 4.28% | −12.50% |
| 15 | 63.4039 | 2.89% | 66.5861 | 3.03% | 5.02% |
| 16 | 186.6146 | 8.50% | 200.2029 | 9.12% | 7.28% |
| 17 | 229.3778 | 10.45% | 258.1879 | 11.77% | 12.56% |
| 18 | 162.6473 | 7.41% | 152.4821 | 6.95% | −6.25% |
| 19 | 96.4034 | 4.39% | 91.3826 | 4.16% | −5.21% |

Table 8: Comparison with classical centrality measures

| graph / accuracy | betweenness | closeness | Shapley value | Myerson value |
|---------------------|-------------|-----------|---------------|---------------|
| karate-34 | 100% | 50% | 100% | 100% |
| karate-empty-34 | 100% | 50% | 100% | 100% |
| karate-karate-34 | 100% | 50% | 100% | 100% |
| karate-star-34 | 100% | 100% | 100% | 100% |
| karate-twoStar-34 | 100% | 50% | 100% | 50% |
| karate-cycle-34 | 100% | 100% | 100% | 100% |
| karate-twoClique-34 | 0% | 0% | 100% | 100% |
| karate-complete-34 | 0% | 0% | 100% | 100% |

4.3 Network properties with opinion dynamics experiments description

We have done simulations of opinion dynamics in one-layer Zachary’s karate club network and two-layer network with Zachary’s karate club network being external layer and different internal structures. There are internal layers we use in our analysis:

1. **karate**: Zachary’s karate club network;
2. **star**: star structure with node 0 being the center;
3. **two-star**: two central nodes 0 and 17, nodes 1–16 are linked with node 0, nodes 18–33 are linked with node 17. Moreover, nodes 0 and 17 are linked;
4. **cycle**: node 0 is linked with node 1, node 1 is linked with node 2, and so on. Finally, node 33 is linked with node 0;
5. **two-clique**: nodes 0–16 belong to the first clique, nodes 17–33 belong to the second clique, and these two cliques are connected through link between nodes 0 and 17;
6. **complete**: all nodes are linked with each other.

We start with simulations of opinion dynamics of BVM, and then CVM and GCVm implementing different internal structures and their affect on consensus time and winning rate. Network properties (in this paper, centrality measurements) will also change with changes in the network structure.

4.4 Network properties with opinion dynamics experiments results

Fig. 3a shows how internal average shortest path d_I varies with the network structure.⁵ Fig. 3b shows how internal density varies with the network structure.

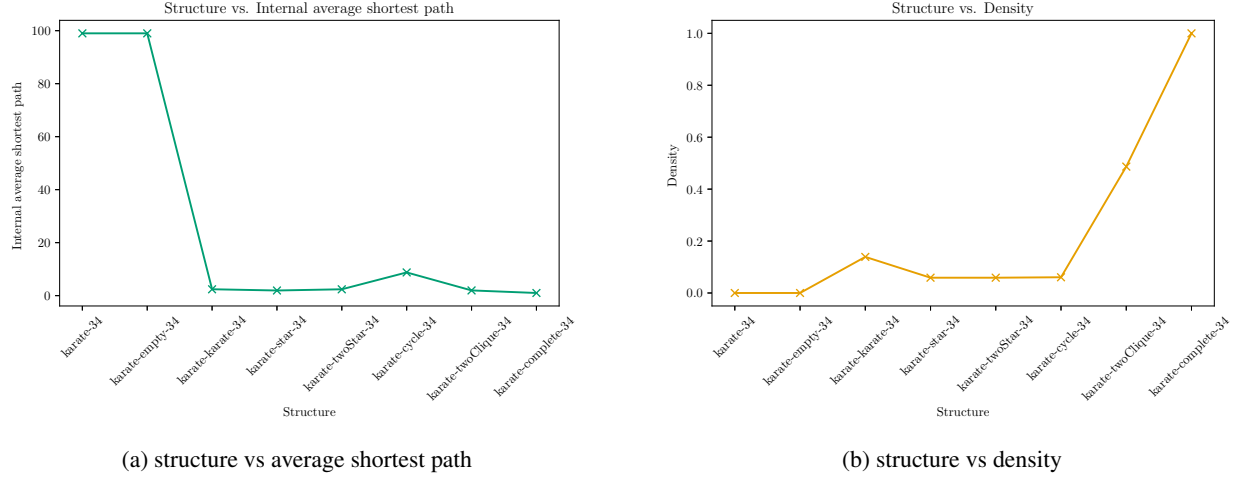


Figure 3: Internal average shortest path and density for different structures

Fig. 4 shows the different centralities for different network structures. In the left of Fig. 4, we show the betweenness centrality, closeness centrality, approximated Shapley value, and approximated Myerson value for Node 0 and Node 33 on our simplified one layer weighted network. And in the right one, we show the group degree centrality, group closeness centrality, group betweenness centrality and two different random walk centralities for the two-layer network with different internal structures.

Fig. 5 shows how KPIs vary with different network structures. Looking at Fig. 4, we may notice that some centralities trend of Node 33 are very similar to the trend in Fig. 3a. Fig. 3b also demonstrates exactly the same trend as in Fig. 5b.

Fig. 5a shows that the structure has a great impact on winning rate, but we have not yet found reasonable explanations for this.

We conducted correlation tests on the above observation results by SciPy [57, 58]. Correlation coefficients are presented in Table 9 (*, **, * * * after the correlation coefficients represent the level of significance 0.05, 0.01, 0.001 respectively).

From Table 9 we can see that:

1. *High positive correlations:* (i) The internal density D_I exhibits a very strong positive correlation with consensus time across all correlation methods (Pearson, Kendall, and Spearman), with coefficients above 0.95, highly significant (* * *). This indicates that as D_I increases, the T_{cons} significantly increases. (ii) d_I is significantly positively correlated with most centrality measures under the methods Kendall and Spearman, and the correlations are generally strong.
2. *Negative correlations:* T_{cons} shows strong negative correlations with network centrality measures like Betweenness and Closeness, especially with Closeness (-0.928 * *), suggesting that higher centrality scores are associated with shorter T_{cons} . It's reasonable in the real life, that very authoritative nodes can result in a faster consensus.
3. *Variability in correlations:* Different metrics show varying levels of correlation strength across the Pearson, Kendall, and Spearman methods. This variability indicates that the strength and significance of correlations can depend on the correlation method used, likely influenced by the underlying data distributions.

⁵“Karate-34” and “karate-empty-34” refer to a one-layer Zachary’s karate club network and to a two-layer network with Zachary’s karate club network in external layer and empty internal layer respectively (i.e. d_I does not exist for these two structures, in particular, it is equal to infinity. But in Fig. 3a, we use a value of 99 instead of infinity).

⁶We choose node 33 as the input for centrality. Actually, if we choose another node as input, the conclusion is still valid.

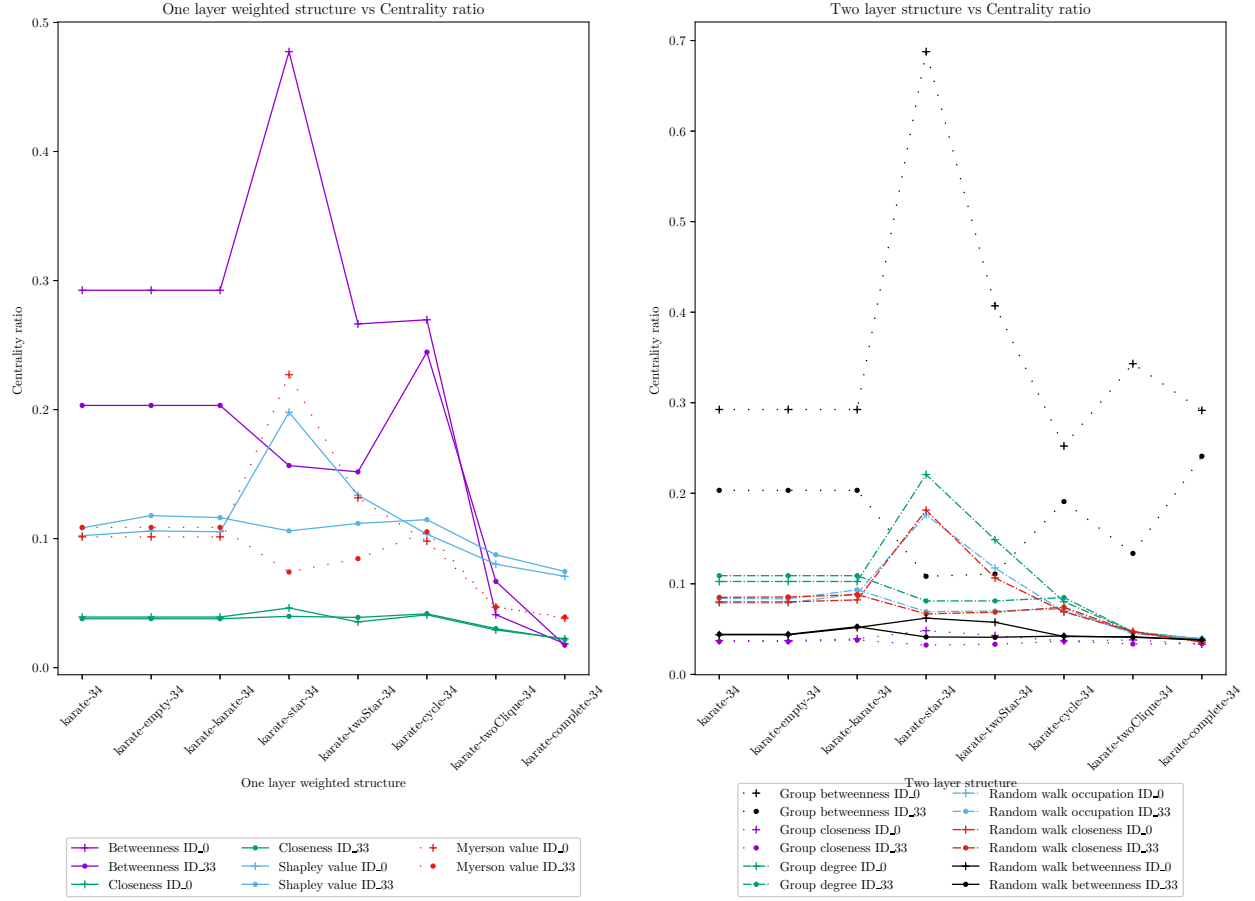
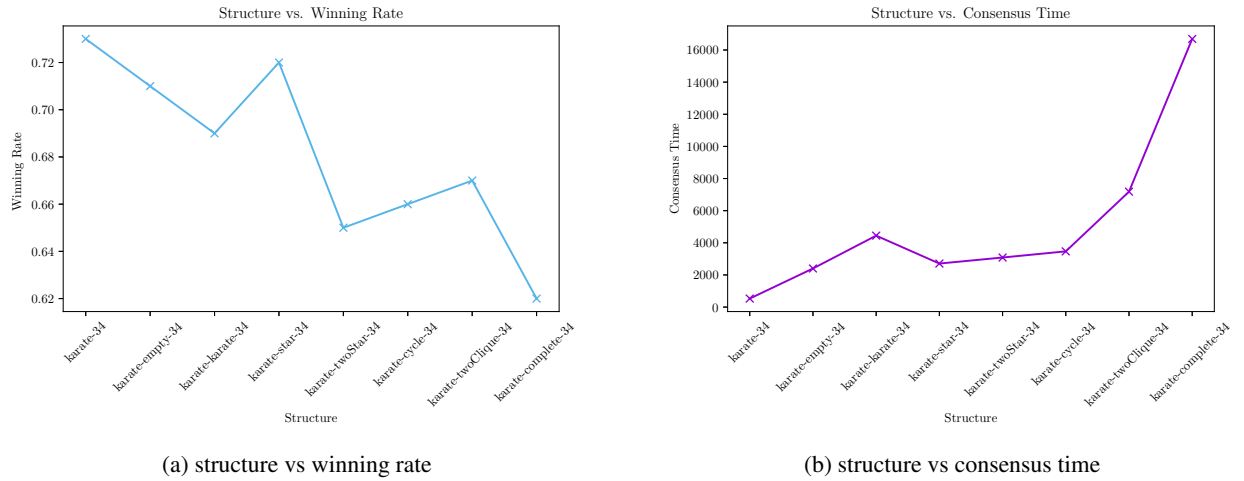


Figure 4: Different centralities for different structures



(a) structure vs winning rate

(b) structure vs consensus time

Figure 5: Winning rate and consensus time for different structures

In summary, Table 9 highlights significant relationships between specific network properties and metrics like consensus time. Centrality of authoritative nodes and the density of network playing a crucial role in influencing the consensus time.

Table 9: Correlation coefficients

| Comparison | Pearson [59] | Kendall [60] | Spearman [61] |
|---------------------------------------|--------------|--------------|---------------|
| d_I vs Betweenness | 0.414 | 0.654* | 0.810* |
| d_I vs Closeness | 0.231 | 0.192 | 0.270 |
| d_I vs Shapley value | 0.363 | 0.618* | 0.766* |
| d_I vs Myerson value | 0.548 | 0.808** | 0.908** |
| d_I vs Group betweenness | 0.366 | 0.185 | 0.157 |
| d_I vs Group closeness | 0.408 | 0.333 | 0.614 |
| d_I vs Group degree | 0.610 | 0.830** | 0.933*** |
| d_I vs Random walk occupation | 0.475 | 0.691* | 0.826* |
| d_I vs Random walk closeness | 0.553 | 0.691* | 0.826* |
| d_I vs Random walk betweenness | 0.161 | 0.618* | 0.778* |
| T_{cons} vs Betweenness | -0.841** | -0.491 | -0.537 |
| T_{cons} vs Closeness | -0.928*** | -0.340 | -0.464 |
| T_{cons} vs Shapley value | -0.872** | -0.286 | -0.452 |
| T_{cons} vs Myerson value | -0.791* | -0.491 | -0.659 |
| T_{cons} vs Group betweenness | 0.407 | 0.255 | 0.299 |
| T_{cons} vs Group closeness | -0.291 | 0.109 | 0.036 |
| T_{cons} vs Group degree | -0.807* | -0.593* | -0.771* |
| T_{cons} vs Random walk occupation | -0.785* | -0.429 | -0.548 |
| T_{cons} vs Random walk closeness | -0.834* | -0.357 | -0.524 |
| T_{cons} vs Random walk betweenness | -0.424 | -0.500 | -0.571 |
| D_I vs T_{cons} | 0.983*** | 0.964** | 0.988*** |

5 Conclusions and future work

We examined opinion dynamics models including BVM, CVM, and GCV in Zachary’s karate club. In CVM and GCV, we assume different structures of the internal layer and conduct simulations for all these internal layers. We examined how internal network structure affects consensus time and winning rate, and if these KPIs correlate with network centrality measures.

We proposed two fast and accurate centrality measurement algorithms based on game-theoretic approach. Our algorithms can effectively approximate theoretical values and operate at high speeds. Both of our algorithms can identify the most important nodes in the network. The sampling concept in our algorithm can be easily transferred to other fields, such as explainable artificial intelligence.

We think the following developments of our work are interesting: (i) incorporating stubbornness and redefining consensus conditions to observe the impact of stubbornness on KPIs, (ii) formalizing consensus time and winning rate, (iii) exploring the reasons of winning rate variation when network structure changes, (iv) get the analytical expression for approximate Shapley/Myerson value based centrality.

Acknowledgments

The work of the second author was supported by Russian Science Foundation grant, grant no. 22-11-00051. <https://rscf.ru/en/project/22-11-00051/>

References

- [1] LW McKeehan. A contribution to the theory of ferromagnetism. *Physical Review*, 26(2):274, 1925.
- [2] Katarzyna Sznajd-Weron and Jozef Sznajd. Opinion evolution in closed community. *International Journal of Modern Physics C*, 11(06):1157–1165, 2000.
- [3] Richard A Holley and Thomas M Liggett. Ergodic theorems for weakly interacting infinite systems and the voter model. *The annals of probability*, pages 643–663, 1975.
- [4] Michael T Gastner, Beáta Oborny, and Máté Gulyás. Consensus time in a voter model with concealed and publicly expressed opinions. *Journal of Statistical Mechanics: Theory and Experiment*, 2018(6):063401, 2018.

- [5] Michael T Gastner, Károly Takács, Máté Gulyás, Zsuzsanna Szvetelszky, and Beáta Oborny. The impact of hypocrisy on opinion formation: A dynamic model. *PLoS one*, 14(6):e0218729, 2019.
- [6] Chi Zhao and Elena Parilina. Opinion dynamics in two-layer networks with hypocrisy. *Journal of the Operations Research Society of China*, 12(1):109–132, Mar 2024. ISSN 2194-6698. doi:10.1007/s40305-023-00503-2. URL <https://doi.org/10.1007/s40305-023-00503-2>.
- [7] Morris H DeGroot. Reaching a consensus. *Journal of the American Statistical Association*, 69(345):118–121, 1974.
- [8] Noah E Friedkin and Eugene C Johnsen. Social influence and opinions. *Journal of Mathematical Sociology*, 15(3-4):193–206, 1990.
- [9] Rainer Hegselmann and Ulrich Krause. Opinion dynamics and bounded confidence models, analysis and simulation. *Journal of Artificial Societies and Social Simulation*, 5, 2002.
- [10] Guillaume Deffuant, David Neau, Frederic Amblard, and Gérard Weisbuch. Mixing beliefs among interacting agents. *Advances in Complex Systems*, 3(01n04):87–98, 2000.
- [11] Sergey E Parsegov, Anton V Proskurnikov, Roberto Tempo, and Noah E Friedkin. Novel multidimensional models of opinion dynamics in social networks. *IEEE Transactions on Automatic Control*, 62(5):2270–2285, 2016.
- [12] Sadegh Bolouki, Roland P. Malhame, Milad Siami, and Nader Motee. Éminence grise coalitions: On the shaping of public opinion. *IEEE Transactions on Control of Network Systems*, 4(2):133 – 145, 2017. doi:10.1109/TCNS.2015.2482218.
- [13] Yulia Kareeva, Artem Sedakov, and Mengke Zhen. Influence in social networks with stubborn agents: From competition to bargaining. *Applied Mathematics and Computation*, 444:127790, 2023. ISSN 0096-3003. doi:<https://doi.org/10.1016/j.amc.2022.127790>. URL <https://www.sciencedirect.com/science/article/pii/S009630032200858X>.
- [14] Vladimir Mazalov and Elena Parilina. The euler-equation approach in average-oriented opinion dynamics. *Mathematics*, 8(3), 2020. ISSN 2227-7390. doi:10.3390/math8030355. URL <https://www.mdpi.com/2227-7390/8/3/355>.
- [15] M.A. Rogov and A.A. Sedakov. Coordinated influence on the opinions of social network members. *Autom Remote Control*, 81:528–547, 2020.
- [16] D. A. Gubanov. Methods for analysis of information influence in active network structures. *Automation and Remote Control*, 83(5):743–754, 2022. doi:10.1134/S0005117922050071.
- [17] D.A. Gubanov and A.G. Chkhartishvili. Influence levels of users and meta-users of a social network. *Automation and Remote Control*, 79(3):545–553, 2018.
- [18] Carmela Bernardo, Claudio Altafini, Anton Proskurnikov, and Francesco Vasca. Bounded confidence opinion dynamics: A survey. *Automatica*, 159:111302, 2024. ISSN 0005-1098. doi:<https://doi.org/10.1016/j.automatica.2023.111302>. URL <https://www.sciencedirect.com/science/article/pii/S0005109823004661>.
- [19] Hossein Noorazar. Recent advances in opinion propagation dynamics: A 2020 survey. *The European Physical Journal Plus*, 135:1–20, 2020.
- [20] Quanbo Zha, Gang Kou, Hengjie Zhang, Haiming Liang, Xia Chen, Cong-Cong Li, and Yucheng Dong. Opinion dynamics in finance and business: a literature review and research opportunities. *Financial Innovation*, 6:1–22, 2020.
- [21] Chi Zhao and Elena Parilina. Consensus time and winning rate based on simulations in two-layer networks with hypocrisy. In *2023 7th Scientific School Dynamics of Complex Networks and their Applications (DCNA)*, pages 68–71, 2023. doi:10.1109/DCNA59899.2023.10290478.
- [22] Vladimir Mazalov and Julia V Chirkova. *Networking games: network forming games and games on networks*. Academic Press, 2019.
- [23] Linton C Freeman. A set of measures of centrality based on betweenness. *Sociometry*, pages 35–41, 1977.
- [24] Alex Bavelas. Communication patterns in task-oriented groups. *The journal of the acoustical society of America*, 22(6):725–730, 1950.
- [25] Linton C. Freeman. Centrality in social networks conceptual clarification. *Social Networks*, 1(3):215–239, 1978. ISSN 0378-8733. doi:[https://doi.org/10.1016/0378-8733\(78\)90021-7](https://doi.org/10.1016/0378-8733(78)90021-7). URL <https://www.sciencedirect.com/science/article/pii/0378873378900217>.
- [26] Gert Sabidussi. The centrality index of a graph. *Psychometrika*, 31(4):581–603, 1966.

- [27] James Powell and Matthew Hopkins. 9 - library networks—coauthorship, citation, and usage graphs. In James Powell and Matthew Hopkins, editors, *A Librarian's Guide to Graphs, Data and the Semantic Web*, Chandos Information Professional Series, pages 75–81. Chandos Publishing, 2015. ISBN 978-1-84334-753-8. doi:<https://doi.org/10.1016/B978-1-84334-753-8.00009-9>. URL <https://www.sciencedirect.com/science/article/pii/B9781843347538000099>.
- [28] Albert Solé-Ribalta, Manlio De Domenico, Sergio Gómez, and Alex Arenas. Random walk centrality in interconnected multilayer networks. *Physica D: Nonlinear Phenomena*, 323:73–79, 2016.
- [29] Mark EJ Newman. A measure of betweenness centrality based on random walks. *Social networks*, 27(1):39–54, 2005.
- [30] Mateusz K Tarkowski, Tomasz P Michalak, Talal Rahwan, and Michael Wooldridge. Game-theoretic network centrality: A review. *arXiv preprint arXiv:1801.00218*, 2017.
- [31] Lloyd S Shapley et al. A value for n-person games. 1953.
- [32] Roger B Myerson. Graphs and cooperation in games. *Mathematics of operations research*, 2(3):225–229, 1977.
- [33] N Rama Suri and Yadati Narahari. Determining the top-k nodes in social networks using the shapley value. In *Proceedings of the 7th international joint conference on Autonomous agents and multiagent systems-Volume 3*, pages 1509–1512, 2008.
- [34] Vladimir V Mazalov, KE Avrachenkov, LI Trukhina, and Bulat T Tsynguev. Game-theoretic centrality measures for weighted graphs. *Fundamenta Informaticae*, 145(3):341–358, 2016.
- [35] Vladimir V Mazalov and VA Khitraya. A modified myerson value for determining the centrality of graph vertices. *Automation and Remote Control*, 82:145–159, 2021.
- [36] VA Khitraya and VV Mazalov. Game-theoretic centrality of directed graph vertices. *AUTOMATION AND REMOTE CONTROL*, 85(2), 2024.
- [37] Paolo Boldi and Sebastiano Vigna. Axioms for centrality. *Internet Mathematics*, 10(3-4):222–262, 2014.
- [38] Chi Zhao and Elena M. Parilina. Network structure properties and opinion dynamics in two-layer networks with hypocrisy. In Anton Ereemeev, Michael Khachay, Yury Kochetov, Vladimir Mazalov, and Panos Pardalos, editors, *Mathematical Optimization Theory and Operations Research*, pages 300–314, Cham, 2024. Springer Nature Switzerland. ISBN 978-3-031-62792-7.
- [39] Ginestra Bianconi. *Multilayer networks: structure and function*. Oxford university press, 2018.
- [40] Ch. Zhao and E. M. Parilina. Analysis of consensus time and winning rate in two-layer networks with hypocrisy of different structures. *Vestnik of Saint Petersburg University. Applied Mathematics. Computer Science. Control Processes*, 20(2):170–192, 2024. doi:10.21638/11701/spbu10.2024.204.
- [41] Wayne W Zachary. An information flow model for conflict and fission in small groups. *Journal of anthropological research*, 33(4):452–473, 1977.
- [42] Dense graph - wikipedia. https://en.wikipedia.org/wiki/Dense_graph. (Accessed on 02/20/2024).
- [43] Martin G Everett and Stephen P Borgatti. The centrality of groups and classes. *The Journal of mathematical sociology*, 23(3):181–201, 1999.
- [44] Martin G Everett and Stephen P Borgatti. Extending centrality. *Models and methods in social network analysis*, 35(1):57–76, 2005.
- [45] Junzhou Zhao, John CS Lui, Don Towsley, and Xiaohong Guan. Measuring and maximizing group closeness centrality over disk-resident graphs. In *Proceedings of the 23rd International Conference on World Wide Web*, pages 689–694, 2014.
- [46] Fan RK Chung. *Spectral graph theory*, volume 92. American Mathematical Soc., 1997.
- [47] Mark Newman. *Networks: An Introduction*. Oxford University Press, 03 2010. ISBN 9780199206650. doi:10.1093/acprof:oso/9780199206650.001.0001. URL <https://doi.org/10.1093/acprof:oso/9780199206650.001.0001>.
- [48] Karen Stephenson and Marvin Zelen. Rethinking centrality: Methods and examples. *Social networks*, 11(1):1–37, 1989.
- [49] Linton C Freeman, Stephen P Borgatti, and Douglas R White. Centrality in valued graphs: A measure of betweenness based on network flow. *Social networks*, 13(2):141–154, 1991.
- [50] L. Lovász. Random walks on graphs: A survey. *Combinatorics, Paul Erdos is Eighty*, 2(1):1–46, 1993. URL http://scholar.google.de/scholar.bib?q=info:llcRghStI1oJ:scholar.google.com/&output=citation&hl=de&as_sdt=0,5&ct=citation&cd=3.

- [51] Zhongzhi Zhang, Alafate Julaiti, Baoyu Hou, Hongjuan Zhang, and Guanrong Chen. Mean first-passage time for random walks on undirected networks. *The European Physical Journal B*, 84:691–697, 2011.
- [52] John G Kemeny, J Laurie Snell, et al. *Finite markov chains*, volume 26. van Nostrand Princeton, NJ, 1969.
- [53] Georg Pólya. Eine wahrscheinlichkeitsaufgabe in der kundenwerbung. *Zamm-zeitschrift Fur Angewandte Mathematik Und Mechanik*, 10:96–97, 1930. URL <https://api.semanticscholar.org/CorpusID:123056679>.
- [54] Matthew O Jackson et al. *Social and economic networks*, volume 3. Princeton university press Princeton, 2008.
- [55] Vladimir V Mazalov and Lyudmila I Trukhina. Generating functions and the myerson vector in communication networks. *Discrete Mathematics and Applications*, 24(5):295–303, 2014.
- [56] Stanley Milgram. The small world problem. *Psychology today*, 2(1):60–67, 1967.
- [57] scipy.stats.pearsonr — scipy v1.12.0 manual. <https://docs.scipy.org/doc/scipy/reference/generated/scipy.stats.pearsonr.html>. (Accessed on 02/11/2024).
- [58] Pauli Virtanen, Ralf Gommers, Travis E. Oliphant, Matt Haberland, Tyler Reddy, David Cournapeau, Evgeni Burovski, Pearu Peterson, Warren Weckesser, Jonathan Bright, Stéfan J. van der Walt, Matthew Brett, Joshua Wilson, K. Jarrod Millman, Nikolay Mayorov, Andrew R. J. Nelson, Eric Jones, Robert Kern, Eric Larson, C J Carey, İlhan Polat, Yu Feng, Eric W. Moore, Jake VanderPlas, Denis Laxalde, Josef Perktold, Robert Cimrman, Ian Henriksen, E. A. Quintero, Charles R. Harris, Anne M. Archibald, Antônio H. Ribeiro, Fabian Pedregosa, Paul van Mulbregt, and SciPy 1.0 Contributors. SciPy 1.0: Fundamental Algorithms for Scientific Computing in Python. *Nature Methods*, 17:261–272, 2020. doi:10.1038/s41592-019-0686-2.
- [59] STUDENT. PROBABLE ERROR OF A CORRELATION COEFFICIENT. *Biometrika*, 6(2-3):302–310, 09 1908. ISSN 0006-3444. doi:10.1093/biomet/6.2-3.302. URL <https://doi.org/10.1093/biomet/6.2-3.302>.
- [60] Maurice G Kendall. The treatment of ties in ranking problems. *Biometrika*, 33(3):239–251, 1945.
- [61] Charles Spearman. The proof and measurement of association between two things. *The American journal of psychology*, 100(3/4):441–471, 1987.